Thermally induced structural evolution of methylsilicone xerogel monoliths reinforced by titania nanoparticles

Huifang Xu · Li Liu · Haijiao Zhang ·
Qiuyang Chen · Wei Dong · Yudong Huang ·
Haifeng Guo

Abstract Thermally stable methylsilicone xerogel monoliths were prepared by sol–gel technology with methylsilicone oligomer as precursor and titania nanoparticles as filler. The effects of titania doping and heating temperature on the structure, morphology, and hydrophobic property of xerogels were investigated. The structural evolution under thermal treatment showed that the blank methylsilicone monolith was crushed after 300 °C treatment, but the samples reinforced by titania could retain the intact structure after 500 °C treatment. Thermogravimetric analysis results certified that the thermal degradation of methylsilicone was resisted due to incorporation of TiO_2. Fourier transform infrared spectra and ^{29}Si nuclear magnetic resonance results showed that Si–CH_3 unit still existed in the reinforced samples, compared with the complete transformation of Si–C to Si–O in the blank methylsilicone after 500 °C treatment. Thus, the hydrophobic property was preserved and certified by measurement of contact angle.

H. Xu (✉) · L. Liu · Q. Chen · W. Dong · Y. Huang (✉)
School of Chemical Engineering and Technology, Harbin
Institute of Technology, Harbin 150001, China
e-mail: xuhf@hit.edu.cn

Y. Huang
e-mail: ydhuang.hit1@aliyun.com

H. Zhang
Engineering Institute of Graphite New Materials, Heilongjiang
University of Science and Technology, Harbin 150027, China

H. Guo
PetroChina pipeline R&D center, Langfang, Hebei 065000,
China

Introduction

Porous materials prepared by sol–gel technology, including ordered porous material, aerogels and xerogels, have been widely investigated for their application in the fields of catalysis, adsorption, heat resistance, and depollution [1–3]. The sol–gel reaction parameters, such as optimized reactant ratio, temperature, solvent, catalyst, and drying procedure, will greatly affect their textural structure [4]. For keeping the porous structure from collapse, supercritical drying is used to form aerogels [5]. Recently, ambient pressure drying has aroused intense attention for the safety and low price. With appropriate treatment, the xerogels derived by ambient drying could have controlled structure and property [6].

As one of important components, silica xerogels have been continually studied and applied because of their well-tailored structure and properties [7–11]. Especially, monolithic silica porous aerogels or xerogels are increasingly investigated due to their easier manipulation and recycle than powder and thin films in the practical application. It is necessary to obtain monolithic porous materials with a fixed shape and structure stability for the specific technical application such as catalyst supports, heat insulator, and recycled adsorbent [12–14]. However, it is still a challenge to keep structure stability of the monolith under complicated condition such as high temperature and moist environment. The important factor among the synthesis procedure is hydrophobic treatment for preserving stability of the porous monolithic structure under ambient drying and avoiding the deterioration under moisture [15–17]. The hydrophobic property could be derived by post treatment with hydrophobic reagent, or copolymerization with hydrophobic precursor. The elastic silica xerogel monoliths have been prepared by copolymerization of tetraalkoxysilane with

organotrialkoxysilane or by direct reaction of organotrialkoxysilane [18]. Methylsilicone, as heat-resistant polymer matrix, was widely used in fabrication of composite materials [19]. Recently, we proposed a facile method to prepare methylsilicone xerogels by one-step gelation reaction [20]. The porous structure and heat-resistant property of the methylsilicone monolith are promising in application of heat insulator. However, the structure stability of the monoliths under high temperature was limited due to the thermal degradation of organic groups [21], which resulted in the loss of monolithic structure and hydrophobic property. Thermal stability of methylsilicone could be enhanced by incorporation of fillers such as polyhedral oligomeric silsesquioxane (POSS) and inorganic oxides [22–24]. For the porous methylsilicone, inorganic nanoparticles had been applied as reinforced fillers to stabilize the monolith [25, 26]. The investigation showed incorporation of fillers in methylsilicone xerogels was efficient on preserving the monolithic structure, but the structural evolution with increased temperature was not clearly revealed.

Herein, TiO_2 nanoparticles, as heat-resistant filler, synthesized by a liquid-phase method, were embedded in methylsilicone matrix. The structural stability of as-prepared monoliths was studied by testing the structural evolution and the hydrophobic property after calcinations. The analyses by SEM, FTIR, N_2 isotherm, XRD, TGA, ^{29}Si-NMR, and contact angle studies showed filling titania in methylsilicone favored the resistance of methylsilicone to oxidation decomposition and stabilized the siloxane structure against thermal oxidation of Si–CH$_3$ to Si–O of the reinforced xerogel monoliths.

Experimental section

Materials

Commercial methylsilicone was purchased from ShangHai Chemical Co. The methylsilicone was a solution with 30 wt% in ethanol. Absolute ethanol, tetrabutyl titanate, ammonia, and nitric acid were used without further purification.

Preparation of methylsilicone xerogel monoliths reinforced by TiO_2

Nanosized TiO_2 was prepared by a modified liquid-phase synthesis method [27]. The typical procedure was as follows: 50 mL tetrabutyl titanate was mixed with 50 mL absolute ethanol. 2 mol/L ammonia was dropped into above mixture till the pH value of the system was about 7–8. The white precipitation was washed, dispersed into 2 mol/L nitric acid solution under stirring, and then reacted

at 60 °C for 4 h to form white slurry. The slurry was washed till the pH value of filter was near 7, and further washed by absolute ethanol to displace the water.

The methylsilicone xerogels were prepared according to our previous report [20]. The composite xerogels were formed by dispersing a calculated amount of TiO_2 in methylsilicone solution under sonication. The gelation of the methylsilicone was catalyzed by ammonia. The gel monoliths were washed by ethanol and dried under ambient conditions. The as-prepared samples with different contents of TiO_2 were denoted as x %TiMSi (x % was the percent of TiO_2 in the composite xerogels). The xerogel monoliths were treated under different temperatures for 30 min to investigate the structural evolution.

Characterization

Scanning electron microscopy measurement (SEM) was performed with a Quanta 200 FEI instrument operated at an accelerating voltage of 30 kV. TGA was performed on a CANY thermoanalyzer (ZRT-2P) in the temperature range of 50–800 °C in air condition at a heating rate 10 °C/min. Transmission electron microscope observation (TEM) was conducted with JEM-2100 electron microscope. Wide-angle X-ray powder diffraction (XRD: Rigaku D/max-2500) was used to characterize the crystalline phase. FTIR were recorded using a Bruker Equinox 55 spectrometer with samples pressed into KBr pellets. ^{29}Si-NMR spectra were tested on a Bruker AV 300 instrument. Nitrogen isotherm was performed on a Micrometritics ASAP 2020M surface area and porosity analyzer. Pore size distributions were obtained by Barret–Joyner–Halenda (BJH) method based on the desorption branch of the nitrogen sorption isotherms. Brunauer–Emmet–Teller (BET) method was used for surface area measurement. Contact angles of the monoliths were measured by a SL200B contact angle meter.

Results and discussion

Preparation of xerogel monolith

The homogeneous distribution of filler in matrix was one of crucial factors for obtaining the structure stability. For improving the dispersion of TiO_2 in methylsilicone matrix, TiO_2 nanoparticles were prepared by an acid peptizing process to form a stable dispersion system. Firstly, hydrolysis and condensation of $Ti(OC_4H_9)_4$ resulted in white precipitation which was peptized in acid aqueous solution to form TiO_2 nanoparticles. The acid peptization resulted in TiO_2 nanoparticles with surface bonding hydroxyl groups [28, 29]. The small particle size and

surface hydroxyl groups promoted the dispersion of TiO$_2$ nanoparticles in the solution of ethanol and methylsilicone oligomer, and prevented the suspension of TiO$_2$ during reaction process. On the other hand, crystalline TiO$_2$ was formed by liquid-phase peptization in strong acid aqueous solution. The crystalline phases were dependent on the reaction parameters. The high acidity will favor the formation of thermostable rutile phase [30]. However, the excess amount of acid used in peptization process will cause difficulty in removal of acid solution in TiO$_2$ suspension and influence the gelation reaction of methylsilicone. Thus, the acid concentration in this study was controlled to a relative low value to balance the peptization and cleansing of TiO$_2$ nanoparticles. The synthesized TiO$_2$ was dispersed in methylsilicone oligomer solution under sonication. The gelation was catalyzed by ammonia. After being dried under ambient condition, the intact monoliths were formed. The gelation process was accelerated with increased ammonia concentration and amount, but the excessive ratio of ammonia to methylsilicone led to the crack in the monoliths.

Investigation of structural evolution of xerogel monolith

The structural evolution and stability of the monoliths was tested by heat treatment at different temperatures. The result showed that the blank methylsilicone xerogel monoliths could only withstand the calcination temperature under 300 °C. Although being treated at 500 °C, the xerogels reinforced by TiO$_2$ could retain the initial appearance with negligible shrinkage. The enhanced dimensional stability due to incorporation of TiO$_2$ nanoparticles was investigated by the following analyses. TGA was applied to
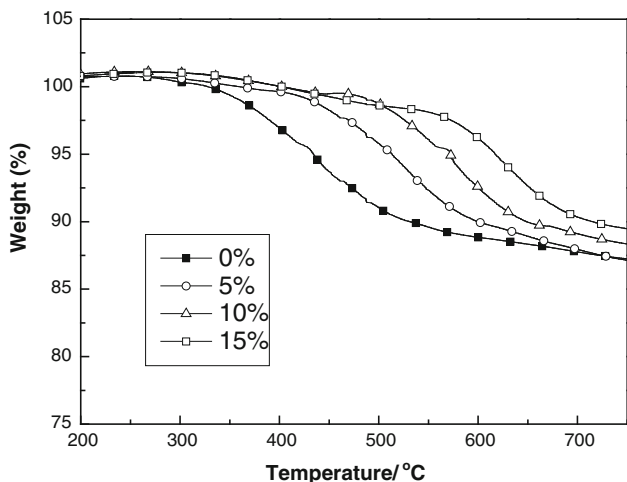
study the thermal properties of the porous monoliths up to 800 °C under air condition. As shown in Fig. 1, two weight-loss stages for all samples were displayed. The weight losses in first step were less than 2 % for all samples. It was reported that the thermal-cured methylsilicone usually lost about 10 % weight during 200–300 °C [31]. The weight-loss mechanisms were proposed due to the elimination of small molecules released by condensation of the unreacted end groups and sublimation of cyclics formed by the hydroxyl chain ends "biting" into the chain a few units back [32]. The low weight-loss in this study indicated the high reaction degree of terminal groups by catalysis of NH$_4$OH. The second step weight-loss due to the thermal oxidation degradation of –CH$_3$. TGA results indicated that the initial and maximum weight-loss temperatures of the second step were delayed with increasing TiO$_2$ contents, showing the improved thermal stability of
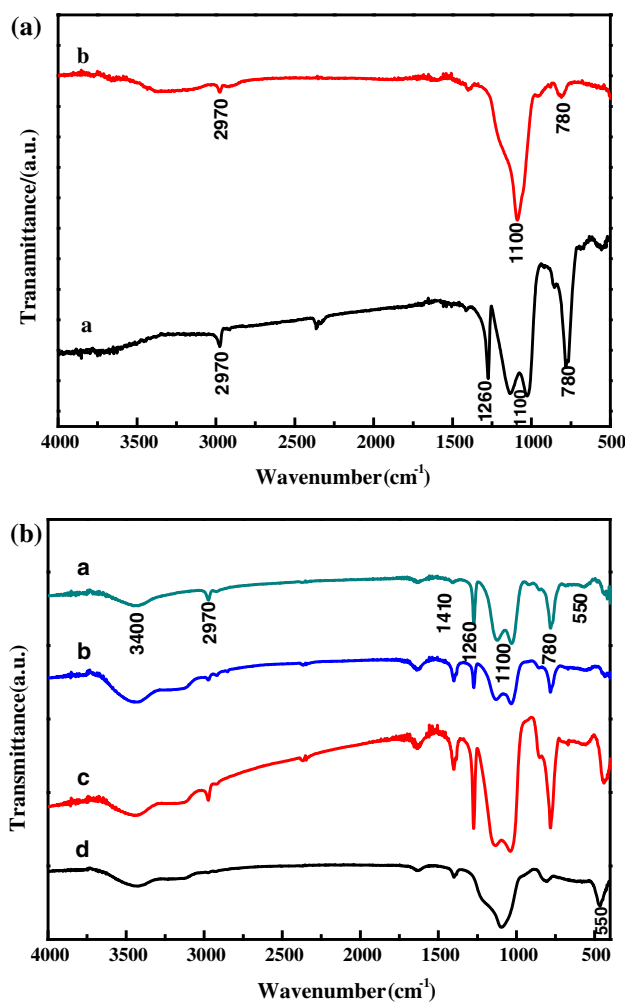
Fig. 2 FTIR spectra. **A**: *a* Methylsilicone; *b* Methylsilicone treated at 300 °C. **B**: FTIR spectra of 15 %TiMSi treated at different temperatures. *a* as-prepared sample; *b* treated at 400 °C; *c* treated at 500 °C; and *d* treated at 600 °C

Fig. 1 TGA of methylsilicone and methylsilicone reinforced with different percentages of TiO$_2$

TiO$_2$-reinforced samples. For the blank methylsilicone, the second weight-loss stage started at about 370 °C, resulting in the macroscopic crush of the monolith when treated at 500 °C. The second degradation temperatures of 5 %TiMSi, 10 %TiMSi, and 15 %TiMSi were about 449, 520, and 577 °C, and the maximum degradation temperature were 512, 566, and 610 °C, respectively. Apparently, incorporation of TiO$_2$ in methylsilicone mainly stabilized the second-stage degradation of methylsilcone, corresponding to the reaction of organic groups. In was deduced that incorporation of TiO$_2$ into methylsilicone retarded polymer chain motion, caused by interaction between TiO$_2$ and methylsilicone chain [33].

The evolution of chemical structure of the samples was first studied by FTIR in Fig. 2. Fig. 2A shows the structural change of methylsilicone xerogel. It was revealed that the characteristic organic groups at 1260 cm^{-1} (Si–C) and 2970 cm^{-1} (C–H) almost disappeared after 300 °C treatment, and curve b was similar to inorganic silica structure. The results indicated that Si–C structure was broken and changed into Si–O bonds after 300 °C treatment. The
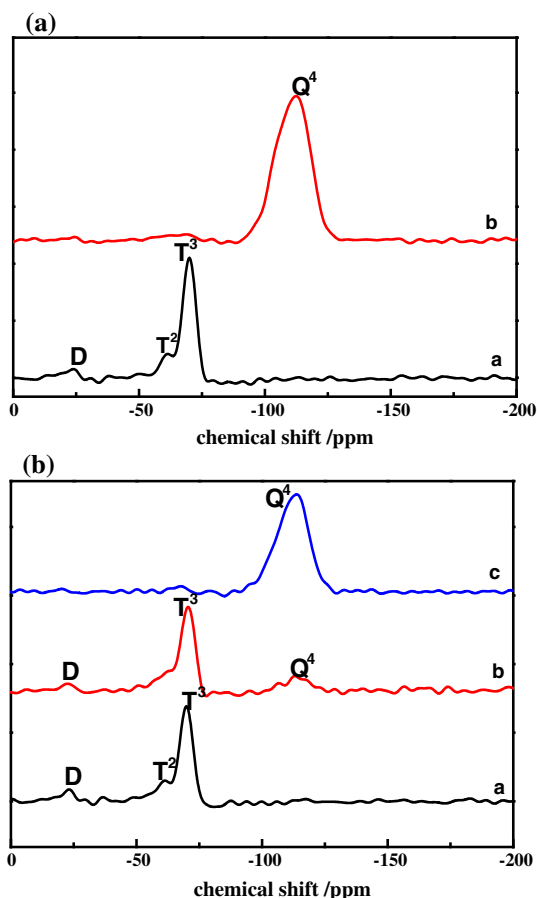
typical TiO$_2$-reinforced sample was treated at different temperatures to observe the transformation of the chemical groups in Fig. 2B. It was found that for a typical sample of 15 %TiMSi, the absorption peaks at 1260 and 2970 cm^{-1} ascribed to Si–C and C–H still existed till 500 °C, revealing that the thermal stability of TiO$_2$-reinforced sample was better than the blank methylsilicone xerogels. When being treated at 600 °C, the absorptions of organic groups were not observed, and only the absorption peaks of Si–O–Si structure were shown. The results were consistent with the macroscopic structural evolution with increased temperature.

^{29}Si-NMR was further used to investigate the silicon surrounding before and after heat treatment. The spectra a in Fig. 3A and 3B showed three bands at about −23.9,
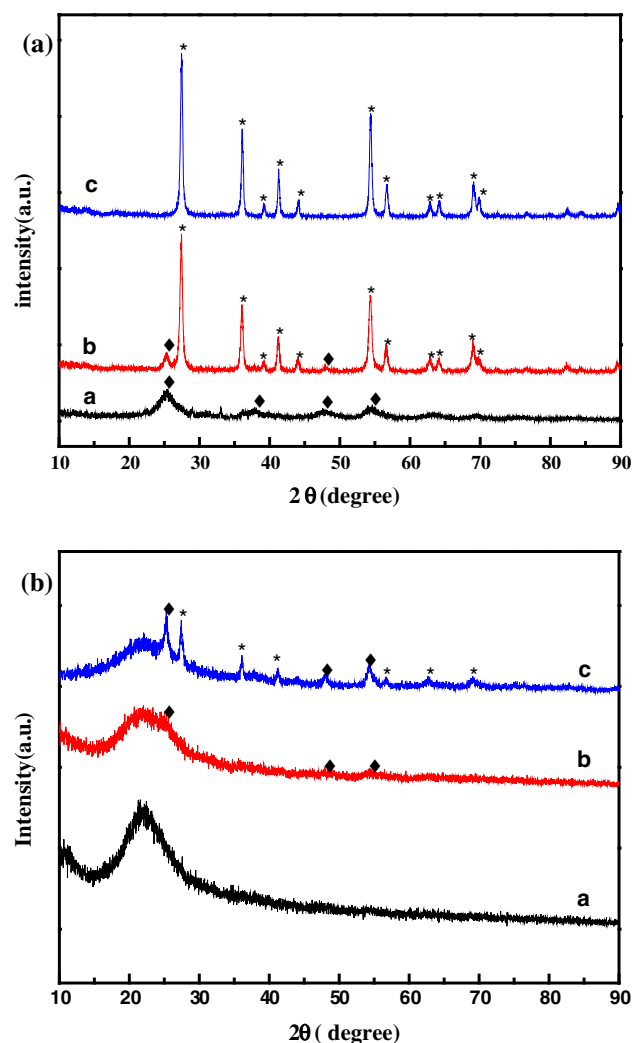

Fig. 3 ^{29}Si-NMR spectra. **A** *a* as-prepared methylsilicone; *b* after 300 °C treatment. **B** *a* as-prepared 15 %TiMSi; *b* 15 %TiMSi after 500 °C treatment; and *c* 15 %TiMSi after 600 °C treatment

Fig. 4 XRD patterns. **A** *a* as-prepared TiO$_2$; *b* TiO-$_2$ after 500 °C treatment; and *c* TiO-$_2$ after 600 °C treatment. **B** *a* as-prepared 15 %TiMSi; *b* 15 %TiMSi after 500 °C treatment; and *c* 15 %TiMSi after 1000 °C treatment. *Filled diagonal* represent anatase phase (JCPDS-No.21-1272) * represent rutile phase(JCPDS-No.21-1276)

Fig. 5 TEM images. **a** TEM and the inset SAED of as-prepared TiO_2; **b** HRTEM of as-prepared TiO_2; **c** TEM and the inset SAED of TiO_2 after 500 °C treatment; **d** HRTEM of anatase phase of TiO_2 after 500 °C treatment with a (101) lattice spacing of 0.348 nm; **e** HRTEM of rutile phase of TiO_2 after 500 °C treatment with a (110) lattice spacing of 0.320 nm; **f** HRTEM of as-prepared 15 %TiMSi; and **g** HRTEM and the inset SAED of 15 %TiMSi after 500 °C treatment
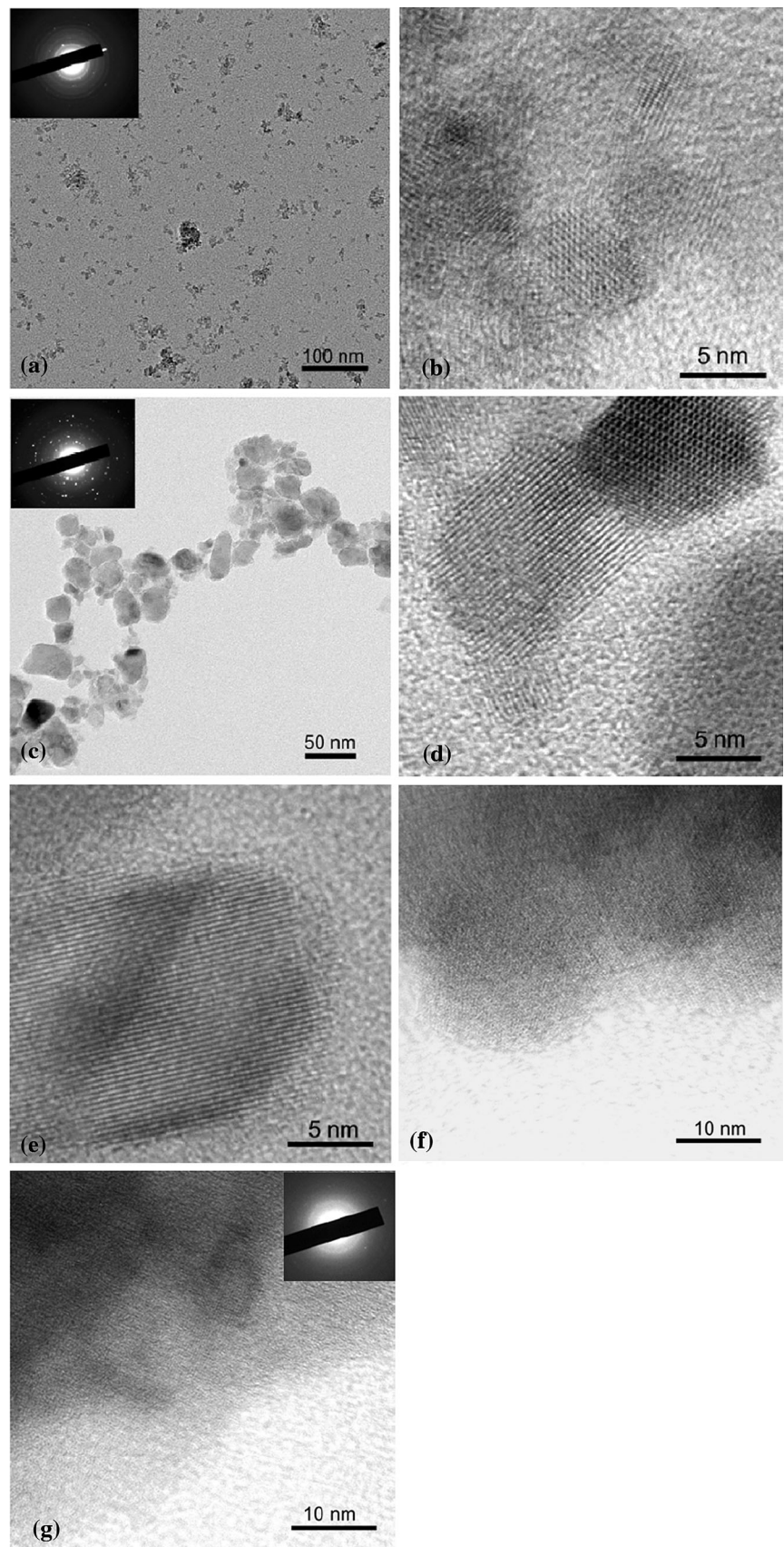
−61.1 and −69.9 ppm which were accorded with D [$SiO_2(CH_3)_2$], T^2 and T^3 units [34], where T^n indicated the siloxane unit structures $RSi(OSi)_nX_{3-n}$ [n = 2(T^2) and 3(T^3);R = Me;X = OH, OR]. The results revealed the as-prepared methylsilicone xerogels and TiO_2-reinforced methylsilicone xerogels were composed by $CH_3Si(OSi)_3$, and a small amount of $SiO_2(CH_3)_2$ and $CH_3Si(OSi)_2OH/CH_3Si(OSi)_2OR$. After heat treatment, ^{29}Si-NMR spectrum b in Fig. 3A revealed that D, T^2, and T^3 structures were transformed into Q^4 structure ($SiO_{4/2}$) at −112.4 ppm when blank methylsilicone xerogel was treated after 300 °C. Spectrum b in Fig. 3B revealed that after 500 °C treatment, 15 %TiMSi was mainly comprised of T^3 structure and a low ratio of Q^4, and T^2 structure had disappeared. The structural transformation to complete Q^4 was retarded to 600 °C. The NMR analyses showed that heating procedure led to elimination of end groups Si–OH and Si–OR, and oxidation of –CH_3 at higher temperature. The comparison certified that TiO_2 filling in methylsilicone favored the resistance of methylsilicone to oxidation decomposition and stabilized the siloxane structure against thermal oxidation of Si–CH_3 to Si–O.

XRD was carried out to reveal the crystalline transformation of TiO_2 and TiO_2-reinforced samples. In Fig. 4A, pattern a showed the diffraction peaks of as-prepared TiO_2 nanoparticles at 2θ of 25.3°, 38.0°, 47.7°, and 54.8° which were assigned to the diffraction planes of (101), (004), (105), and (204) corresponding to anatase phase (JCPDS-No.21-1272). The broad diffraction peaks indicated the nanosized crystals were prepared. However, the dramatic crystalline improvement and phase transformation were observed when the as-prepared TiO_2 was calcined at 500 °C. Mixed anatase and rutile phases were obtained from pattern b of Fig. 4A with rutile phase diffraction peaks occurring at 2θ = 27.4°(110), 36.0°(101), 39.2°(200), 41.2°(111), 44.1°(210), 54.3°(211), 56.6°(220), 64.0°(310), 65.5°(221), and 69.8°(112) (JCPDS-No.21-1276). Most of anatase phase was transformed into rutile, and the diffraction peaks became narrow, revealing the growth of the crystals after calcination. The complete phase transformation from anatase to rutile was achieved at 600 °C.

XRD patterns of 15 %TiMSi are shown in Fig. 4B. Pattern a showed that only a broad diffraction band around 22.0° was ascribed to methylsilicone. The anatase phase could not be observed, because the weak diffraction peak of anatase was overlapped by silicone matrix. Pattern b showed the weak peaks at 25.3°, 47.7°, and 54.8° corresponding to anatase phase. Compared with the blank TiO_2, anatase phase in TiO_2-reinforced methylsilicone xerogel was stable up to 500 °C, and the crystal growth was suppressed. The crystallization was enhanced after being treated at 1000 °C with coexistence of anatase and rutile

phases. Compared with the complete transformation of as-prepared TiO_2 to rutile phase under 600 °C treatment, the phase transformation of TiO_2 in 15 %TiMSi was greatly retarded because the methylsilicone matrix separated and prevented TiO_2 from aggregation and growth.

TEM and High-resolution TEM (HRTEM) were used to compare the structural evolution of as-prepared TiO_2 and the reinforced samples. TEM image of Fig. 5a revealed that the particle size of as-prepared TiO_2 was about 20 nm. Selected area electron diffraction (SAED) pattern in inset showed five fringe patterns with spacing of 0.348, 0.238, 0.186, 0.164, and 0.145 nm, which were consistent with the anatase (101), (004), (200), (211), and (204) spacings. The corresponding HRTEM in Fig. 5b revealed a (101) lattice spacing of 0.348 nm identified as anatase phase. Fig. 5c exhibits the growth of TiO_2 particles to about 30–40 nm after calcination at 500 °C. SAED in inset showed the diffraction patterns of both anatase and rutile, indicating the crystalline phase evolution happened. The
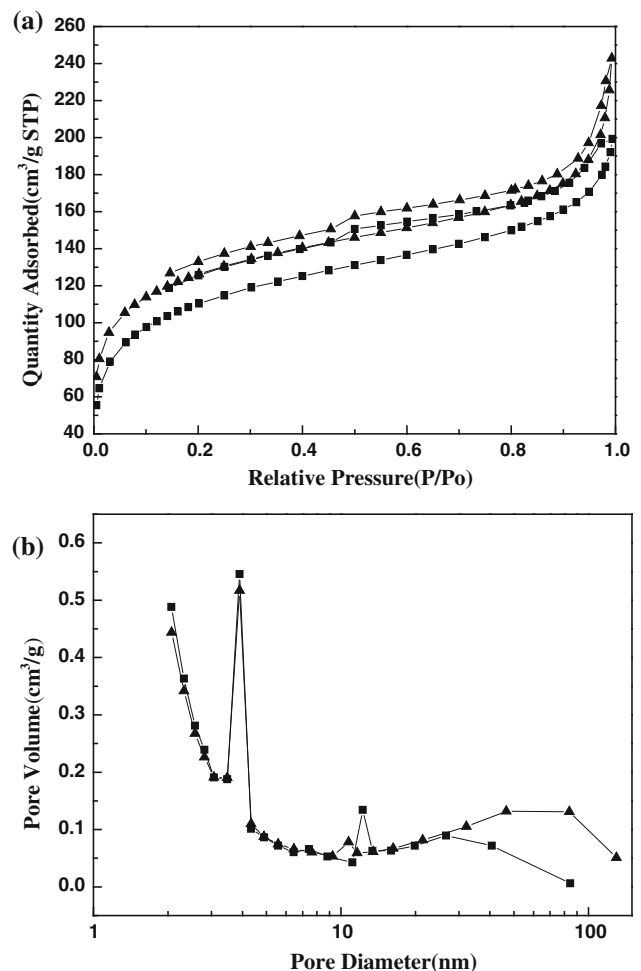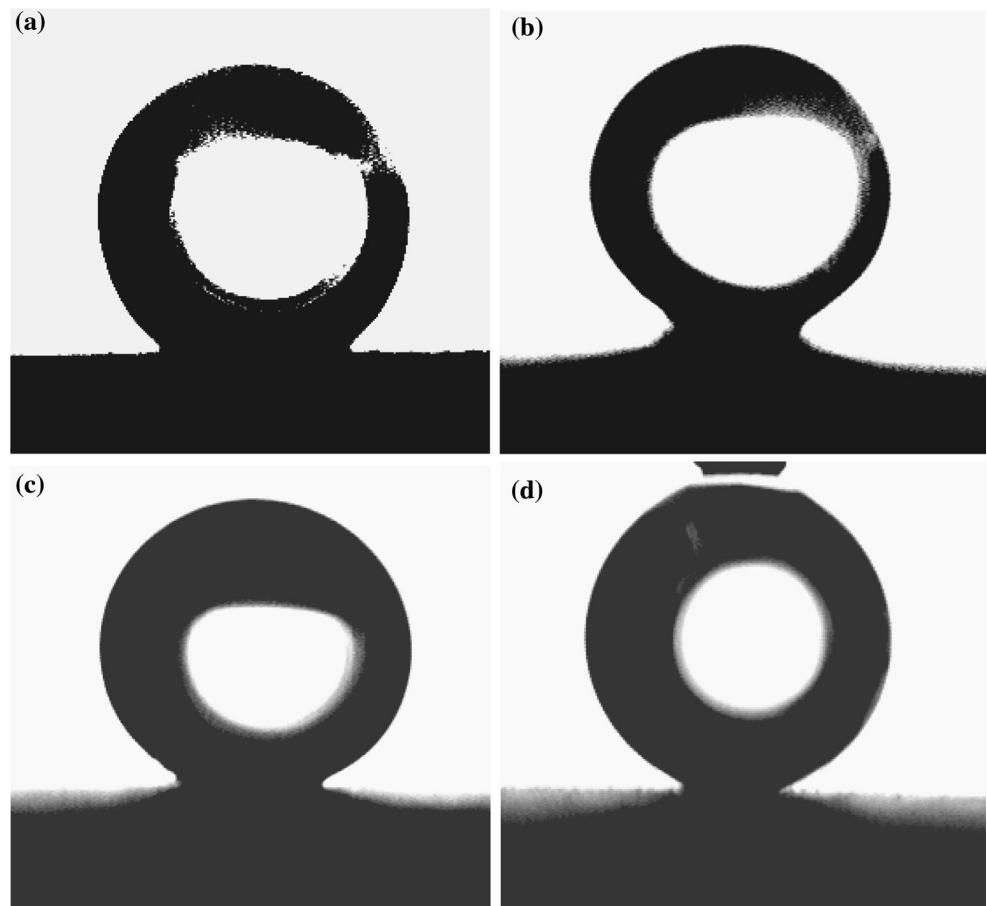

Fig. 6 a Nitrogen adsorption–desorption isotherms; **b** Pore size distribution curves. *Filled square* as-prepared 15 %TiMSi; *filled triangle* 15 %TiMSi after 500 °C treatment

Fig. 7 Contact angles:
a 5 %TiMSi; **b** 15 %TiMSi;
c 5 %TiMSi treated at 500 °C;
and **d** 15 %TiMSi treated at
500 °C

corresponding HRTEM in Fig. 5d and e displayed the (101) lattice spacing of 0.348 nm as anatase phase TiO_2 and rutile phase with a (110) lattice spacing of 0.320 nm, respectively. In HRTEM of 15 %TiMSi showed in Fig. 5f, it was difficult to observe the TiO_2 nanoparticles because they were embedded in methylsilicone matrix. Fig. 5g shows that TiO_2 crystalline lattice was still difficult to be discerned after heat treatment at 500 °C. SAED halo revealed the sample was composed by amorphous structure, which also certified that the crystalline TiO_2 particles were dispersed in amorphous methylsilicone matrix, and the crystallization was inhibited due to the insulation of TiO_2 by methylsilicone matrix. HRTEM and SAED measurements were consistent with the results of XRD analyses. The dispersion stability of TiO_2 in methylsilicone matrix in turn favored the structural stability of TiO_2-reinforced methylsilicone monolith.

The structural parameters of specific surface area and pore volume were derived from N_2 adsorption/desorption isotherms. BET model was used for specific surface area measurement. Pore size distributions were obtained by BJH desorption branch of the nitrogen sorption isotherms. As shown in Fig. 6, the isotherms and pore size distribution

curves of the selected TiO_2-reinforced methylsilicone and its calcination product were compared. Both isotherms exhibited narrow hysteresis loops and uptake in low P/P_0, indicating the existence of mesopores and micropores. The rapid increase of adsorption capacity at P/P_0 near 1.0 revealed the existence of interparticle macropores. The BET surface areas were slightly increased from 392.4 to 443.2 m^2/g after heating at 500 °C. Evidently, the calcination process did not alter the textural structures of TiO_2-reinforced sample, because the significant changes in structural properties such as specific surface area, pore size distribution, and isotherm did not occur as shown in Fig. 6.

The study on hydrophobic property

The hydrophobic property was necessary to avoid crush of porous monoliths due to adsorption of moisture. Especially, for high temperature applications such as heat insulator, it was crucial to keep the hydrophobic property after heat treatment for reserve and recycled application. The wettability was tested by measuring the contact angle of water droplet on the surface of a monolith, shown in Fig. 7. Two typical TiO_2-reinforced methylsilicone xerogels were

investigated. The contact angles of as-prepared 5 %TiMSi and 15 %TiMSi were 142.1° and 156.3°, and the contact angles of the corresponding 500 °C heating samples were 151.9° and 162.7°, respectively, revealing the hydrophobic property was increased after heat treatment. The increased contact angle was due to the elimination of unreacted Si–OH and the reservation of Si–CH$_3$ group, which was certified by the results of FTIR and ^{29}Si-NMR.

For testing their stability under moisture, a piece of monolith was put on water for a period of time. The weight change with time was negligible. The results showed that heat treatment at 500 °C can not influence the monolithic structure and hydrophobic property of TiO$_2$-reinforced methylsilicone xerogel.

Conclusions

In this article, the structural evolution of methylsilicone and TiO$_2$-reinforced methylsilicone composite xerogels under heat treatment was investigated. The results indicated that the structure of the composite xerogels depended on the amount of TiO$_2$ addition. When the temperature was up to 300 °C, porous methylsilicone monolith was crushed. The samples reinforced by TiO$_2$ can resist 500 °C treatment. XRD and TEM showed the crystalline growth and transformation of TiO$_2$ in the doped methylsilicone were delayed. The results of FTIR and ^{29}Si-NMR showed that the organic structural units of pure methylsilicone completely changed into inorganic Q^4 structure units after 300 °C treatment. The TiO$_2$-reinforced methylsilicone was mainly composed of T^3 units after 500 °C treatment, and preserved the intact monolithic structure and hydrophobic property. The study indicated that TiO$_2$-reinforced methylsilicone xerogels, with the thermal stability and hydrophobic property, are promising candidates to be used in the areas of catalysis and heat insulation at as high as 500 °C temperature.

References

1. Yang ZL, Niu ZW, Cao XY, Yang ZZ, Lu YF, Hu ZB, Han CC (2003) Template synthesis of uniform 1D mesostructured silica materials and their arrays in anodic alumina membranes. Angew Chem Int Ed 42:4201–4203

2. Lin KF, Lebedev OI, Tendeloo GV, Jacobs PA, Pescarmona PP (2010) Titanosilicate beads with hierarchical porosity:synthesis and application as epoxidation catalysts. Chem Eur J 16:13509–13518

3. Li XY, Chen LH, Li Y, Rooke JC, Deng Z, Hu ZY, Liu J, Krief A, Yang XY, Su BL (2012) Tuning the structure of a hierarchically porous ZnO$_2$ for dye molecule. Micropor Mesopor Mater 152:110–121

4. Brinker CJ, Scherer GW (1990) Sol–gel Science. Academic Press, New York

5. Bommel MJ, Haan AB (1994) Drying of silica gels with supercritical carbon dioxide. J Mater Sci 29:943–948

6. Harreld JH, Ebina T, Tsubo N, Stucky G (2002) Manipulation of pore size distributions in silica and ormosil gels dried under ambient pressure conditions. J Non Cryst Solids 298(2):241–251

7. Amlouk A, MirL El, Kraiem S, Saadoun M, Alaya S, Pierre AC (2008) Luminescence of TiO$_2$:Pr nanoparticles incorporated in silica aerogel. Mater Sci Eng B 146:74–79

8. Rao AV, Pajonk GM, Parvathy NN (1994) Effect of solvents and catalysts on monolithicity and physical properties of silica aerogels. J Mater Sci 29:1807–1817

9. Tang Q, Xu Y, Wu D, Sun Y (2006) A study of carboxylic-modified mesoporous silica in controlled delivery for drug famotidine. J Solid State Chem 179(5):1513–1520

10. Rao AV, Hegde ND, Hirashima H (2007) Absorption and desorption of organic liquids in elastic superhydrophobic silica aerogels. J Colloid Interface Sci 305(1):124–132

11. Schmidt M, Schwertfeger F (1998) Applications for silica aerogel products. J Non Cryst Solids 225:364–368

12. Wei TY, Lu SY, Chang YC (2009) A new class of opacified monolithic aerogels of ultralow high-temperature thermal conductivities. J Phys Chem C 113:7424

13. Hwang S, Hyun S (2004) Capacitance control of carbon aerogel electrodes. J Non Cryst Solids 347:238–245

14. Li W, Pröbstle H, Fricke J (2003) Electrochemical behavior of mixed C$_m$RF based carbon aerogels as electrode materials for supercapacitors. J Non Cryst Solids 325:1–5

15. Sarawade PB, Kim JK, Hilonga A, Quang DV, Kim HT (2011) Synthesis of hydrophilic and hydrophobic xerogels with superior properties using sodium silicate. Micropor Mesopor Mater 139:138–147

16. Rao AV, Bhagat SD, Hirashima H, Pajonk GM (2006) Synthesis of flexible silica aerogels using methyltrimethoxysilane (MTMS) precursor. J Colloid Interface Sci 300:279–285

17. Janamori K, Aizawa M, Nakanishi K, Hanada T (2007) New transparent methylsilsesquioxane aerogels and xerogels with improved mechanical properties. Adv Mater 19:1589–1593

18. Rao AV, Kalesh RR (2003) Hydrophobicity and physical properties of TEOS based silica aerogels using phenyltriethoxysilane as a synthesis component. J Mater Sci 38:4407–4413

19. Jovanovic JD, Govedarica MN, Dvornic PR, Popovic IG (1998) The thermogravimetric analysis of some polysiloxanes. Polym Degrad Stab 61:87–93

20. Xu HF, Huang YD, Liu L, Song JW, Wang CQ, Zhang LC (2010) Superhydrophobic and porous methylsilicone monoliths prepared by one-step ammonia-catalyzed gelation and ambient pressure drying. J Non Cryst Solids 356:1837–1841

21. Grassie N, Murray EJ, Holmes PA (1984) The thermal degradation of poly(-(D)-β-hydroxybutyric acid): part 2-Changes in molecular weight. Polym Degrad Stab 6:95–103

22. Liu YR, Huang YD, Liu L (2007) Thermal stability of POSS/ methylsilicone nanocomposites. Compos Sci Technol 67:2864–2876

23. Min CY, Huang YD, Liu L (2007) Effect of nanosized ferric oxide on the thermostability of methylsilicone resin. J Mater Sci 42:8695–8699

24. Sim LC, Ramanan SR, Ismail H, Seetharamu KN, Goh TJ (2005) Thermal characterization of Al$_2$O$_3$ and ZnO reinforced silicone rubber as thermal pads for heat dissipation purposes. Thermochim Acta 430:155–165

25. Xu HF, Zhang CH, Zhang HJ, Song JW, Huang YD, Lv T (2011) The preparation and structural characterization of ambient-dried porous methylsilicone matrix doped with SiO_2 powder. J Non Cryst Solids 357:2822–2825

26. Xu HF, Huang YD, Zhang HJ, Chen QY, Yan GW, Liu L (2012) Preparation and characterization of monolithic methylsilicone xerogels doped with liquid-phase synthesized TiO_2. J Non Cryst Solids 358:2922–2926

27. Yang SF, Liu YH, Guo YP, Zhao JZ, Xu HF, Wang ZC (2002) Preparation of rutile titania nanocrystals by liquid method at room temperature. Mater Chem Phys 77:501–506

28. Yu JC, Yu J, Zhao J (2002) Enhanced photocatalytic activity of mesoporous and ordinary TiO_2 thin films by sulfuric acid treatment. Appl Catal B Environ 36:31–43

29. Jung HS, Shin H, Kim J, Kim JY, Hong KS (2004) In situ observation of the stability of anatase nanoparticles and their transformation to rutile in an acidic solution. Langmuir 20:11732–11737

30. Yin H, Wada Y, Kitamura T, Kambe S, Murasawa S, Mori H, Sakata T, Yanagida S (2001) Hydrothermal synthesis of nano-sized anatase and rutile TiO_2 using amorphous phase TiO_2. J Mater Chem 11:1694–1703

31. LiuYR HuangYD, Liu L (2006) Effect of trisilanolisobutyl-POSS on thermal stability of methylsilicone resin. Polym Degrad Stab 91:2731–2738

32. Thomas TH, Kendrick TC (1969) Thermal analysis of poly-dimethylsiloxanes. I. Thermal degradation in controlled atmospheres. J Polym Sci Part A 2 7:537–549

33. Romo-Uribe A, Mather PT, Haddad TS, Lichtenhan JD (1998) Viscoelastic and morphological behavior of hybrid styryl-based polyhedral oligomeric silsesquioxane (POSS) copolymers. J Polym Sci Part B 36(11):1857–1872

34. Ramzi BH, Sami B, Marie-Christine BS, Makki A, Mohamed NB (2008) Adsorption of silane onto cellulose fibers. II. The effect of pH on silane hydrolysis, condensation, and adsorption behavior. J Appl Polym Sci 108:1958–1968